

**This is a self-archived version of an original article. This version may differ from the original in pagination and typographic details.**

**Author(s):** Al-Majid, Abdullah Mohammed; Haukka, Matti; Soliman, Saied M.; Alamary, Abdullah Saleh; Alshahrani, Saeed; Ali, M.; Islam, Mohammad Shahidul; Barakat, Assem

**Title:** X-ray Crystal Structure and Hirshfeld Analysis of Gem-Aminals-Based Morpholine, Pyrrolidine, and Piperidine Moieties

**Year:** 2021

**Version:** Published version

**Copyright:** © 2020 the Authors

**Rights:** CC BY 4.0

**Rights url:** <https://creativecommons.org/licenses/by/4.0/>

**Please cite the original version:**

Al-Majid, A. M., Haukka, M., Soliman, S. M., Alamary, A. S., Alshahrani, S., Ali, M., Islam, M. S., & Barakat, A. (2021). X-ray Crystal Structure and Hirshfeld Analysis of Gem-Aminals-Based Morpholine, Pyrrolidine, and Piperidine Moieties. *Symmetry*, 13(1), Article 20.  
<https://doi.org/10.3390/sym13010020>

## Article

# X-ray Crystal Structure and Hirshfeld Analysis of Gem-Aminals-Based Morpholine, Pyrrolidine, and Piperidine Moieties

 Abdullah Mohammed Al-Majid <sup>1</sup>, Matti Haukka <sup>2</sup> , Saied M. Soliman <sup>3</sup>, Abdullah Saleh Alamary <sup>1</sup>, Saeed Alshahrani <sup>1</sup>, M. Ali <sup>1</sup>, Mohammad Shahidul Islam <sup>1</sup>  and Assem Barakat <sup>1,3,\*</sup> 

- <sup>1</sup> Department of Chemistry, College of Science, King Saud University, P.O. Box 2455, Riyadh 11451, Saudi Arabia; amajid@ksu.edu.sa (A.M.A.-M.); 436106737@student.ksu.edu.sa (A.S.A.); 436106738@student.ksu.edu.sa (S.A.); maly.c@ksu.edu.sa (M.A.); mislam@ksu.edu.sa (M.S.I.)
- <sup>2</sup> Department of Chemistry, University of Jyväskylä, P.O. Box 35, FI-40014 Jyväskylä, Finland; matti.o.haukka@jyu.fi
- <sup>3</sup> Department of Chemistry, Faculty of Science, Alexandria University, P.O. Box 426, Ibrahimia, Alexandria 21321, Egypt; saeed.soliman@alexu.edu.eg
- \* Correspondence: amarakat@ksu.edu.sa; Tel.: +966-11467-5901; Fax: +966-11467-5992

**Abstract:** The gem-aminals of 1,2-dimorpholinoethane (**1**) and 1-morpholino-3-morpholinium bromide propane (**2**) were synthesized by reaction of two molar ratio of morpholine with the halogenating agents in the presence of basic condition ( $K_2CO_3$ ) in acetone at room temperature (RT) overnight. The structures of the centro-symmetric compound **1** and the morpholinium salt derivative **2** were assigned unambiguously by single crystal X-ray diffraction analysis and compared with the 1,2-di(pyrrolidin-1-yl)ethane **3** and 1,2-di(piperidin-1-yl)ethane **4**. The 1,2-dimorpholinoethane molecule has a center of symmetry at the midpoint of the C–C bond of the ethyl moiety leading to two equivalent halves. It crystallized in monoclinic crystal system and  $P2_1/n$  space group, while the unit cell parameters are determined to be  $a = 6.0430(3)$ ,  $b = 8.0805(3)$ ,  $c = 11.1700(4)$  Å, and  $\beta = 97.475(2)^\circ$  with unit cell volume of  $540.80(4)$  Å<sup>3</sup> and  $Z = 2$  at 170(2) K. The less symmetric analogue **2** crystallized in the lower space group  $P2_1$  with unit cell parameters of  $a = 6.37450(10)$ ,  $b = 11.1378(2)$ ,  $c = 9.6549(2)$  Å, and  $\beta = 93.358(2)^\circ$ , while the unit cell volume is  $684.30(2)$  Å<sup>3</sup> at 120(2) K. Using Hirshfeld analysis, the molecules of **1** are mainly packed by weak N...H (4.2%), O...H (16.8%), and H...H (79.0%) interactions. In contrast, the molecules of **2** are packed by significantly short O...H (14.4%) and Br...H (11.6%) interactions in addition to the relatively long H...H (73.3%) interactions. DFT calculations predicted the molecular geometry of the studied compounds showing a good agreement with the experimental X-ray structures. Due to symmetry considerations, compounds **1**, **3**, and **4** are nonpolar with zero dipole moment, while the less symmetric molecule **2** has a dipole moment of 6.914 Debye. Their electronic aspects, such as natural population charges, HOMO, and LUMO energies as well as the corresponding reactivity descriptors, were also calculated and discussed.

**Keywords:** aminals; morpholine; pyrrolidine; piperidine; X-ray; Hirshfeld analysis; DFT



**Citation:** Al-Majid, A.M.; Haukka, M.; Soliman, S.M.; Alamary, A.S.; Alshahrani, S.; Ali, M.; Islam, M.S.; Barakat, A. X-ray Crystal Structure and Hirshfeld Analysis of Gem-Aminals-Based Morpholine, Pyrrolidine, and Piperidine Moieties. *Symmetry* **2021**, *13*, 20. <https://dx.doi.org/10.3390/sym13010020>

Received: 12 November 2020

Accepted: 23 December 2020

Published: 24 December 2020

**Publisher's Note:** MDPI stays neutral with regard to jurisdictional claims in published maps and institutional affiliations.



**Copyright:** © 2020 by the authors. Licensee MDPI, Basel, Switzerland. This article is an open access article distributed under the terms and conditions of the Creative Commons Attribution (CC BY) license (<https://creativecommons.org/licenses/by/4.0/>).

## 1. Introduction

Aminals (gem-dimainines) linked with a spacer were studied extensively in a wide area of chemistry aspects. Aminals were employed as building blocks for the synthesis of gemini basic ionic liquids. This type of ionic liquids was recently investigated as environmental benign catalysts in organic synthesis due to high chemical and thermal stability with low vapor pressure and low viscosities [1–6].

Indeed, the diamines worked as *N*-donor ligands and chiral auxiliaries with many of metal ions such as Ca [7], Fe [8], Ag [9], Ni [10], Pd [11], and Rh [12], indeed, it explored in various catalyzed protocols and were successively employed as efficient catalysts for

many transformations in organic synthesis. In this aspect, the amins (gem-diamines) have been considered as promising electrophiles in metal-catalyzed nucleophilic addition reactions [13].

Nevertheless, gem-diamines are widely used in medicinal products, because the existence of a lone pair on the nitrogen atom will increase and improve the lipophilicity and the solubility of the pharmaceutical targets [14–16]. Given to the prevalence of diamines, there is a need for doing structure elucidation and also studying their chemical insights [17]. The symmetric as well as asymmetric catalysis, in particular in pharmaceutical industry, are continually seeking for rapid synthetic routes to novel heterocyclic structures for early-stage drug discovery, as well as safe, robust and environmentally friendly routes for large scale production. General tactics for the structure elucidations of the amins based on morpholine, pyrrolidine and piperidine as examples for gem-diamines are discussed in this text (Figure 1).

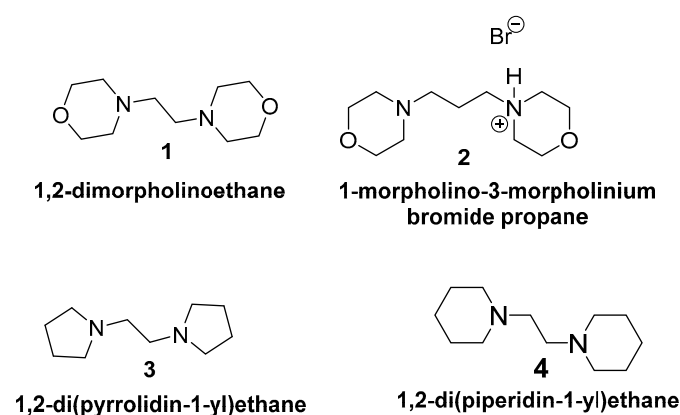


Figure 1. Gem-diamines used in this study.

## 2. Materials and Methods

“The topology analyses were performed using Crystal Explorer 17.5 program [18]. All DFT calculations were performed using Gaussian 09 software package [19,20] utilizing B3LYP/6-31G(d,p) method. Natural charge populations were calculated using NBO 3.1 program as implemented in the Gaussian 09W package [21]”.

### 2.1. Synthesis of 1,2-Dimorpholinoethane 1 and 1-Morpholino-3-Morpholinium Bromide Propane 2

The appropriate morpholine (10 mmol, 870 mg) and  $K_2CO_3$  (11 mmol, 1.520 gm) were stirred in acetone (10 mL) for 1 h, then 1,2-dibromoethane (5 mmol, 935 mg) or 1,3-dibromopropane (5 mmol, 1005 mg) was added followed by continuous stirring overnight.  $K_2CO_3$  in the reaction mixture was removed by simple filtration, and the product was washed with acetone. The solvent was removed under vacuum, and the crystalline compounds were obtained upon standing at room temperature after three and five days for compounds **1** and **2**, respectively.

### 2.2. X-ray Structure Determinations of 1 and 2

The crystals of 1,2-dimorpholinoethane **1** or 1-morpholino-3-morpholinium bromide propane **2** were immersed in cryo-oil, mounted in a loop and measured at a temperature of 170 K in case of **1** and at 120 K for **2**. The X-ray diffraction data were collected on a Bruker Kappa Apex II and Rigaku Oxford Diffraction Supernova diffractometers for the amins **1** and **2**, respectively. The Denzo-Scalepack [22] or CrysAlisPro [23] software packages were used for cell refinements and data reductions for **1** and **2**, respectively. A multi-scan or Gaussian absorption correction based on equivalent reflections (SADABS [24] (**1**) or CrysAlisPro [23] (**2**)) was applied to all data. The structures were solved by intrinsic phasing method using the SHELXT [25] software. Structural refinements were carried

out using *SHELXL* [25] software. In **2**, the NH hydrogen atom was located from the difference Fourier map and refined isotropically. Other hydrogen atoms were positioned geometrically and constrained to ride on their parent atoms, with C-H = 0.99 Å and  $U_{\text{iso}} = 1.2 U_{\text{eq}}$  (parent atom). The structure of **2** was solved in Sohncke space group  $P2_1$ . The Flack parameter was determined to be  $-0.039(9)$ , indicating the presence of just one enantiomer. The crystallographic details are summarized in Table 1.

**Table 1.** Crystal data of 1,2-dimorpholinoethane **1** and 1-morpholino-3-morpholinium bromide propane **2**.

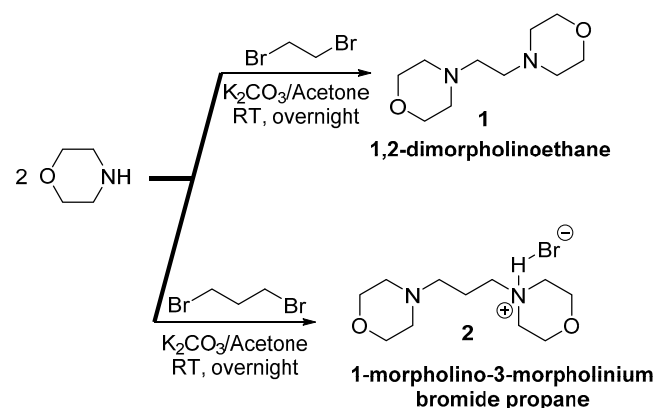
	1	2
empirical formula	$C_{10}H_{20}N_2O_2$	$C_{11}H_{23}BrN_2O_2$
fw	200.28	295.22
temp (K)	170(2)	120(2)
$\lambda$ (Å)	0.71073	1.54184
cryst syst	Monoclinic	Monoclinic
space group	$P2_1/n$	$P2_1$
$a$ (Å)	6.0430(3)	6.37450(10)
$b$ (Å)	8.0805(3)	11.1378(2)
$c$ (Å)	11.1700(4)	9.6549(2)
$\beta$ (deg)	97.475(2)	93.358(2)
$V$ (Å <sup>3</sup> )	540.80(4)	684.30(2)
$Z$	2	2
$\rho_{\text{calc}}$ (Mg/m <sup>3</sup> )	1.230	1.433
$\mu$ (Mo K $\alpha$ ) (mm <sup>-1</sup> )	0.086	4.021
No. reflns.	12461	14253
Unique reflns.	1592	2811
GOOF ( $F^2$ )	1.074	1.054
$R_{\text{int}}$	0.0310	0.0266
$R1^a$ ( $I \geq 2\sigma$ )	0.0419	0.0195
$wR2^b$ ( $I \geq 2\sigma$ )	0.1096	0.0491
CCDC	2,022,360	2,039,255

<sup>a</sup>  $R1 = \sum ||F_o| - |F_c|| / \sum |F_o|$ . <sup>b</sup>  $wR2 = [\sum [w(F_o^2 - F_c^2)^2] / \sum [w(F_o^2)^2]]^{1/2}$ .

### 3. Results

#### 3.1. Chemistry

The aminated compounds 1,2-dimorpholinoethane **1** and 1-morpholino-3-morpholinium bromide propane **2** were synthesized according to Scheme 1 [26–28]. The target compounds proved to be synthesized in high chemical yield (83 and 87% for **1** and **2**, respectively) at room temperature (25 °C). Their chemical features were elucidated based on the single crystal X-ray diffraction analysis.



**Scheme 1.** Synthesis of 1,2-dimorpholinoethane **1** and 1-morpholino-3-morpholinium bromide propane **2**.

### 3.2. X-ray Structure Description of 1 and 2

The X-ray structures of 1 and 2 with atom numbering and thermal ellipsoids drawn at 50% probability level are shown in Figure 2. The aminal 1 as an example for gem-diamine is crystallized in the monoclinic crystal system and centro-symmetric  $P2_1/n$  space group with  $Z = 2$ . The asymmetric unit comprised half molecule due to the presence of inversion center located at the midpoint of the C-C of the ethane moiety. The molecules of 1 in the crystal are packed mainly by weak C5-H5A...O1 interactions leading to the hydrogen bonding network shown in Figure 3.

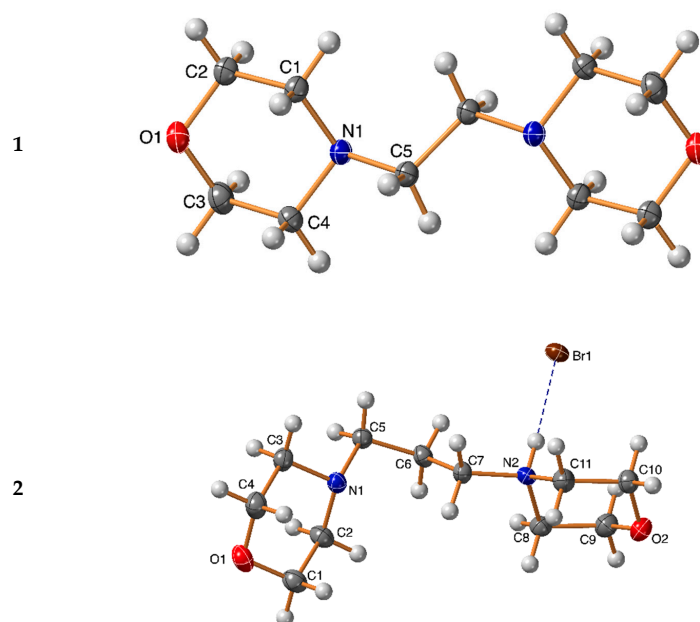


**Figure 2.** X-ray structure showing atom numbering and thermal ellipsoids at 50% probability level for compounds 1 (upper) and 2 (lower).

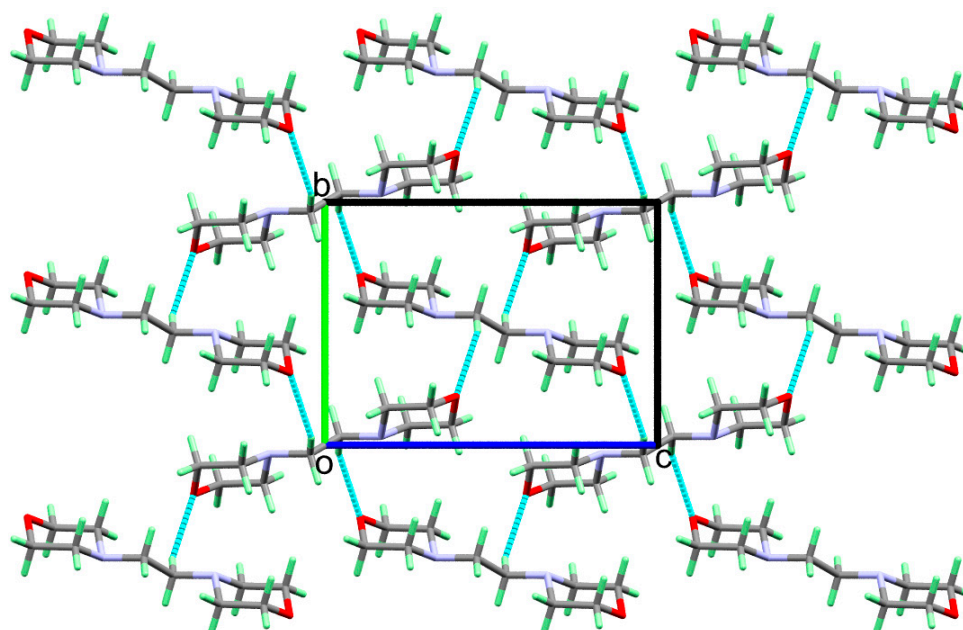


**Figure 3.** Packing of the molecular units in 1 via weak C5-H5A...O1 {C5-H5A: 0.990 Å, H5A...O1: 2.683 Å, C5...O1: 3.577(1) Å, and C5-H5A...O1: 150.2 Å; Symm. code:  $1/2 - x, -1/2 + y, 1/2 - z$ }.

Similarly, **2** crystallized in the monoclinic crystal system and the less symmetric  $P2_1$  space group with  $Z = 2$  and *n*-propyl moiety connecting the morpholine fragments where one of the morpholine moieties comprised a protonated nitrogen site. As a result, the compound is crystallized as 1-morpholino-3-morpholinium bromide propane. In this compound, there is no inversion center at the aliphatic *n*-propyl moiety. The molecular units in the crystal are packed by relatively short N-H...Br hydrogen bonding interactions as well as longer C-H...O and C-H...Br interactions. The details of the hydrogen bond parameters are listed in Table 2. The hydrogen bonding network showing these interactions is shown in Figure 4.

**Table 2.** Hydrogen bond ( $\text{\AA}$ ,  $^\circ$ ) details in **2**<sup>a</sup>.

Atoms	D-H	H...A	D...A	D-H...A
N2-H2...Br1	0.92(3)	2.29(3)	3.205(2)	178(2)
C5-H5B...O1	0.99	2.52	3.457(3)	158
C11-H11B...Br1	0.99	2.75	3.580(3)	142

<sup>a</sup> D: hydrogen bond donor and A: hydrogen bond acceptor.

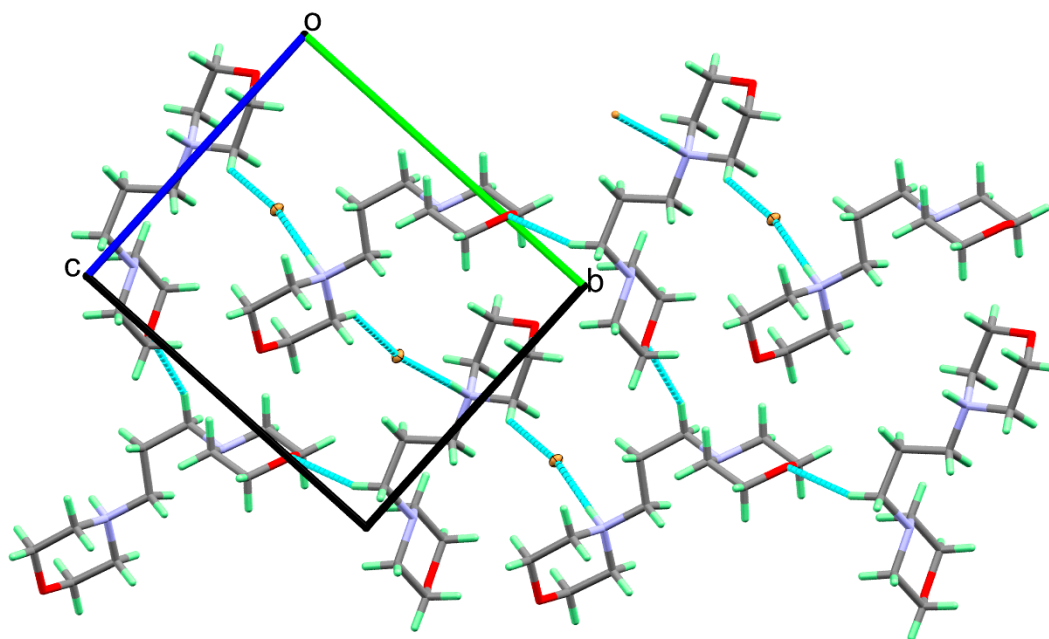


**Figure 4.** Packing of the molecular units in **2**.

### 3.3. Analysis of Molecular Packing

The Hirshfeld surfaces of **1** are shown in Figure 5. The molecules are mainly packed by weak N...H (4.2%), O...H (16.8%), and H...H (79.0%) interactions. The decomposed  $d_{\text{norm}}$  maps and fingerprint plots indicated that all these interactions are weak (Figure 6). All appeared as white or blue regions in the corresponding  $d_{\text{norm}}$  maps, indicating equal or longer distances than the vdW radii sum of the interacting atoms, respectively.

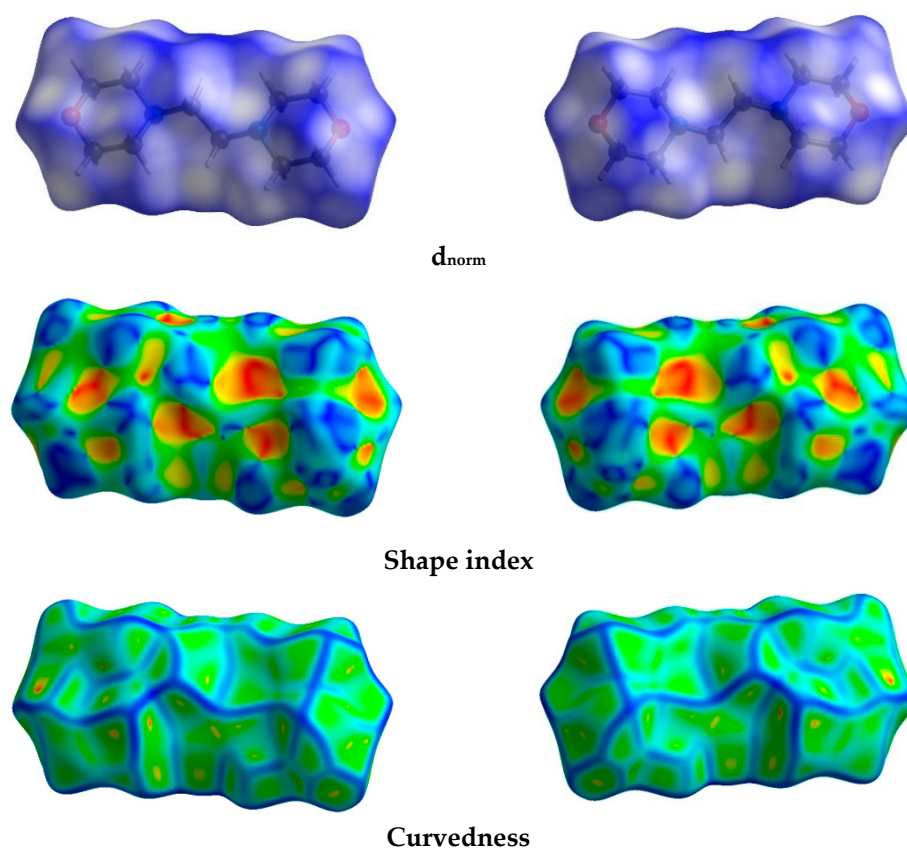
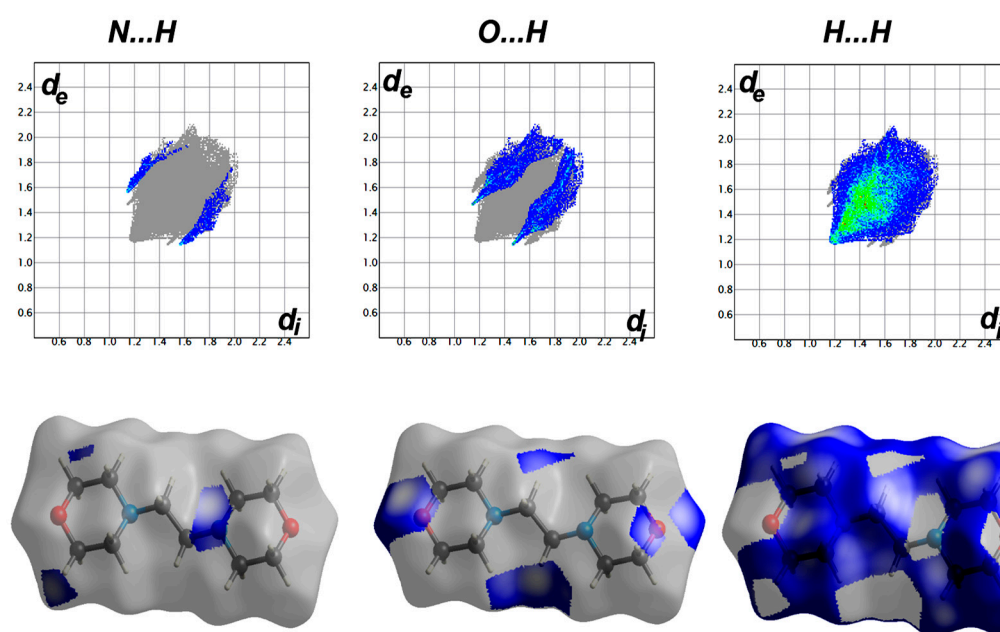


Figure 5. Hirshfeld surfaces of 1.

Figure 6. Fingerprint plots (upper) and  $d_{\text{norm}}$  surfaces (lower) of the N...H, O...H and H...H contacts in 1 ( $d_i$  and  $d_e$  in Å).

Structure CCDC search returned with two structurally related compounds, which are the 1,2-di(pyrrolidin-1-yl)ethane **3** [29] and 1,2-di(piperidin-1-yl)ethane **4** (CCDC: 840298). Their Hirshfeld analyses are presented in Figure 7. Additionally, the molecular packing of **3** is mainly controlled by weak N...H (4.7%) and H...H (95.3%) interactions (Figure 8). Similarly, the packing in case of **4** is dominated by N...H (3.5%) and H...H (96.5%) interactions.

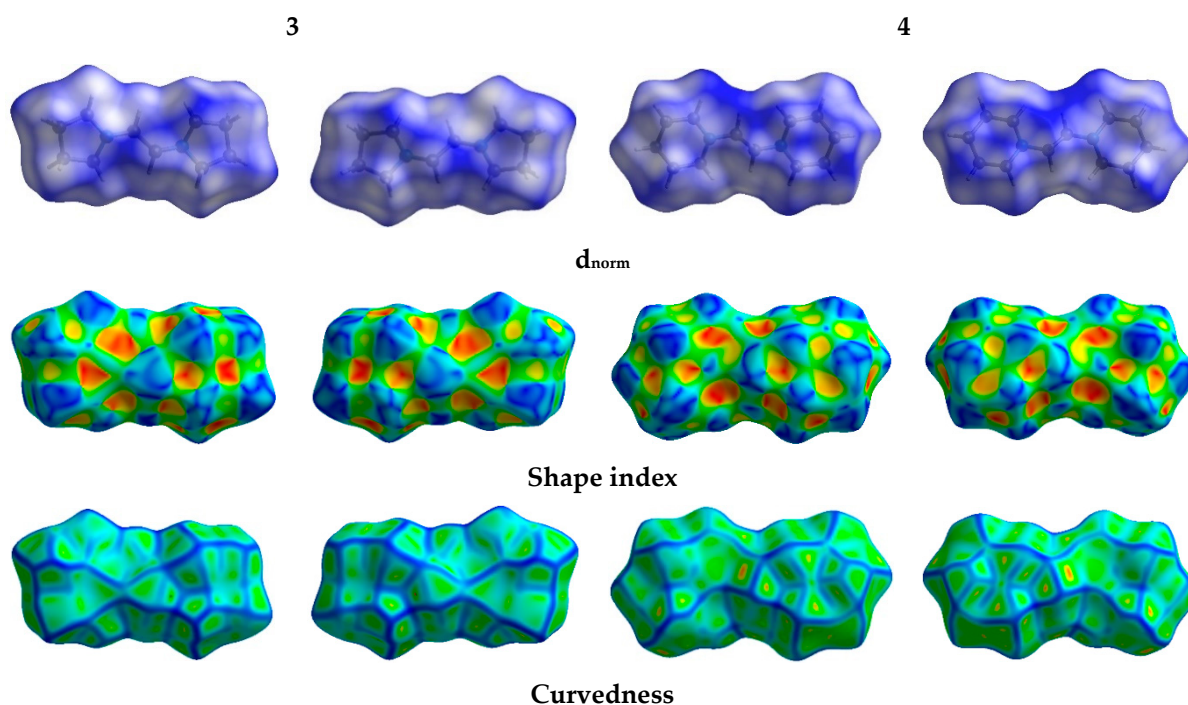


Figure 7. Hirshfeld surfaces of 1,2-di(pyrrolidin-1-yl)ethane **3** and 1,2-di(piperidin-1-yl)ethane **4**.

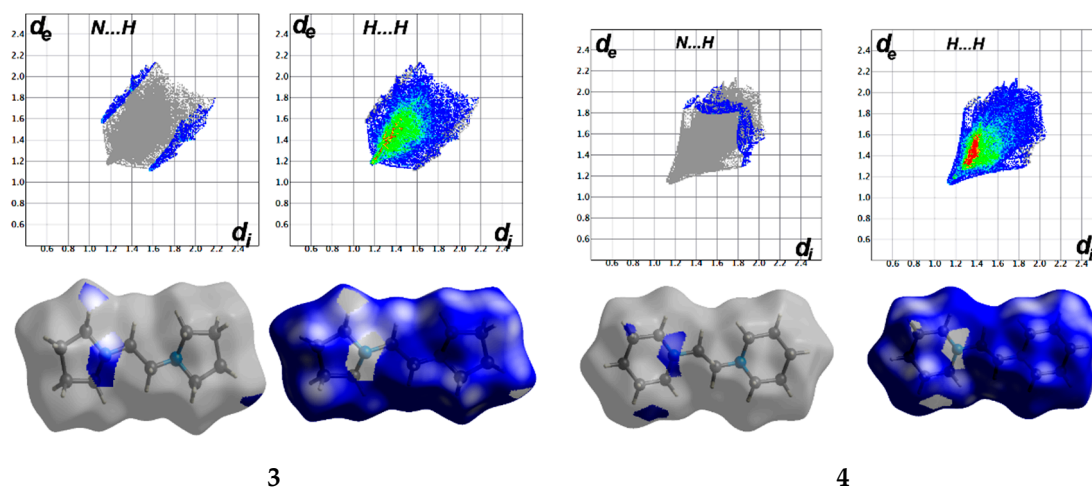


Figure 8. Fingerprint plots (upper) and  $d_{\text{norm}}$  surfaces (lower) of the N...H, and H...H contacts in 1,2-di(pyrrolidin-1-yl)ethane **3** and 1,2-di(piperidin-1-yl)ethane **4** ( $d_i$  and  $d_e$  in Å).

On the other hand, Hirshfeld surfaces of **2** are shown in Figure 9. In contrast to **1**, **3**, and **4**, the molecules of **2** are packed by significantly short O...H (14.4%) and Br...H (11.6%) interactions in addition to the relatively long H...H (73.3%) interactions. The decomposed  $d_{\text{norm}}$  maps showed intense red spots corresponding to these interactions (Figure 9). Additionally, the fingerprint plot has one sharp spike for the Br...H contacts due to the interaction between the N-H proton inside the surface and the bromide anion outside the surface with H...Br distance of 2.197 Å (Br1...H2). On the other hand, the O...H contacts appeared as two relatively sharp spikes, indicating that the surface acting as hydrogen bond donor as well as hydrogen bond acceptor (Figure 10). The shortest O...H contacts are O1...H5B (2.431 Å) and O1...H10B (2.539 Å), while the shortest H...H contact is H1A...H9A (2.281 Å). All these interactions stabilized the crystal structure of the studied molecules, where **2** has a higher melting point than **1** as a consequence of the stronger intermolecular interactions in the former compared to the latter compound.



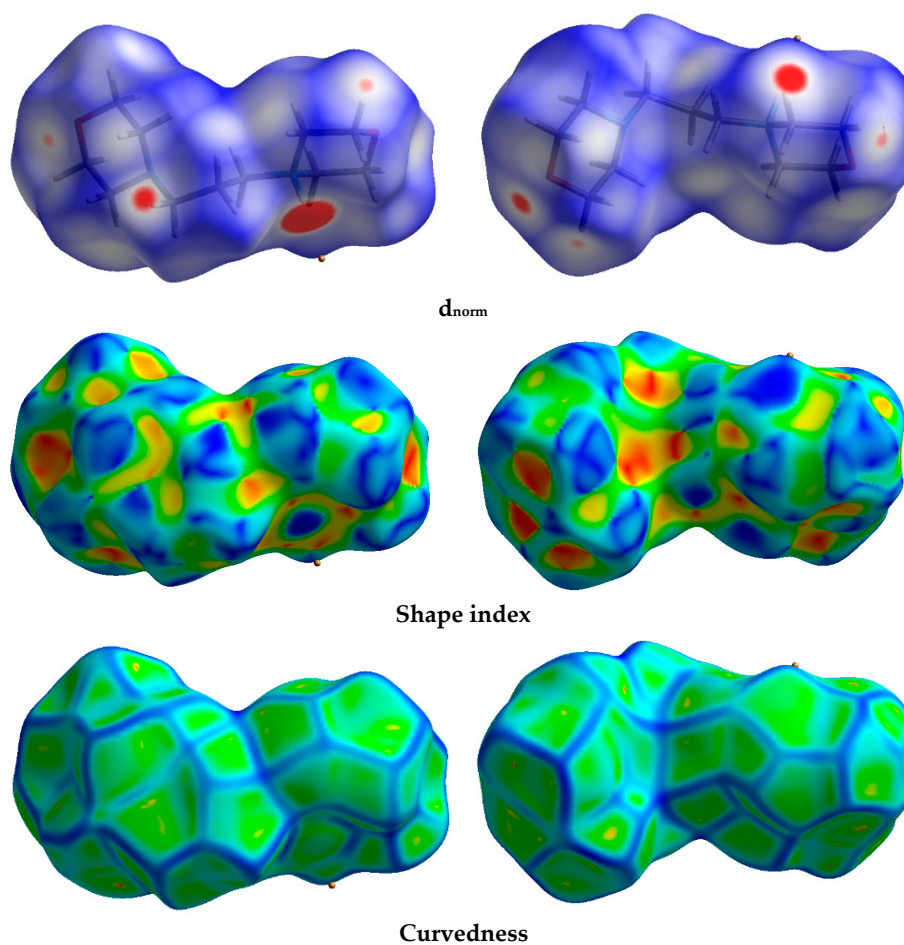
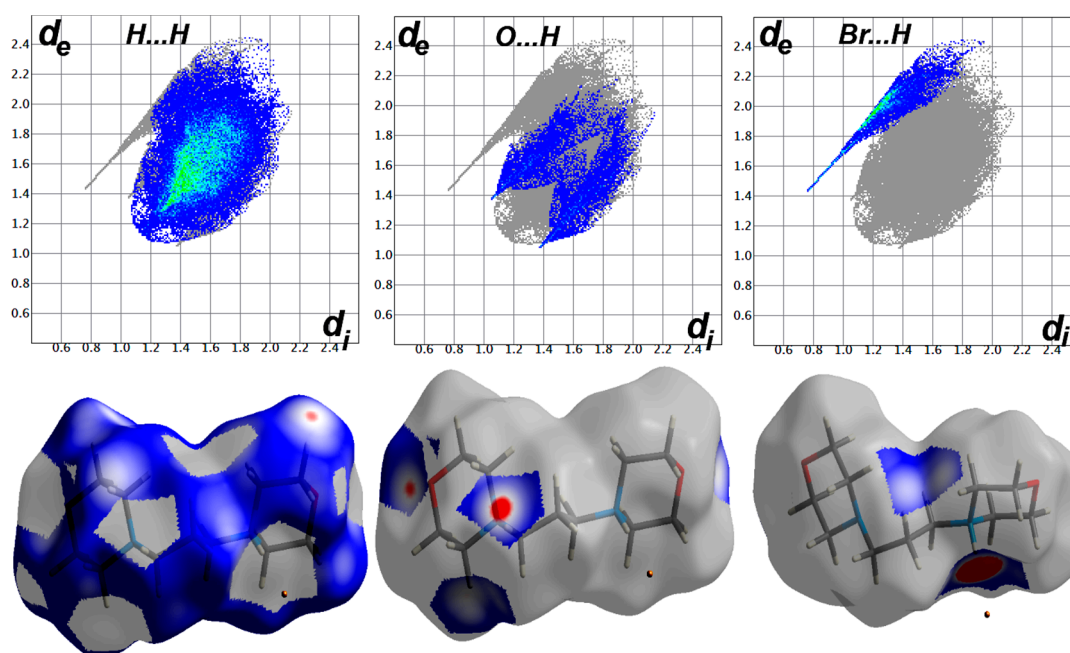
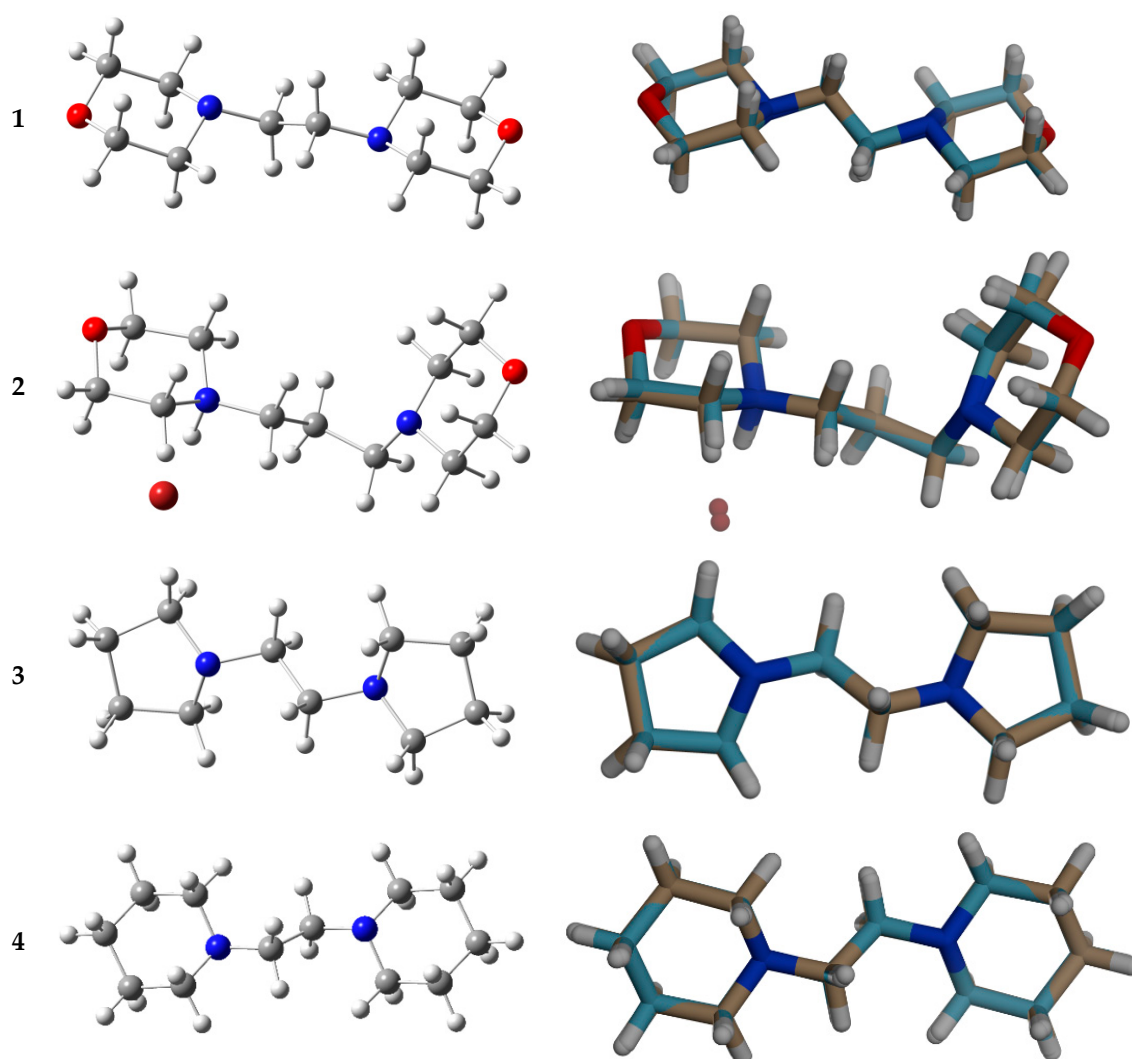


Figure 9. Hirshfeld surfaces of 2.

Figure 10. Fingerprint plots (upper) and  $d_{\text{norm}}$  surfaces (lower) of the Br...H, O...H, and H...H contacts in 2 ( $d_i$  and  $d_e$  in Å).

### 3.4. DFT Studies

The optimized geometries of the studied molecules are presented in Figure 11. Structure matching between the computed molecular geometries with the experimental ones indicated very well the agreement between them (Table S1, Supplementary Materials). The maximum deviations in the bond distances do not exceed 0.013 Å, while for angles, the maximum deviation is 3.2° for **1**. In the case of the 1,2-di(pyrrolidin-1-yl)ethane **3**, the corresponding values are 0.098 Å and 1.5°, respectively, while they are 0.019 Å and 2.46° for **2** and 0.014 Å and 2.9° in **4**, respectively. Generally, the root mean square deviations (RMSD) for bond distances are 0.008, 0.008, 0.027, and 0.007 Å in case of compounds **1–4**, respectively. Due to symmetry considerations, compounds **1**, **3**, and **4** are nonpolar with zero dipole moment, while the less symmetric **2** is polar and has a net dipole moment of 6.914 Debye.



**Figure 11.** The optimized geometries (**left**) and overlay of the optimized with experimental structures (**right**) for the studied molecules.

The partial atomic charges using the NBO method revealed the high electronegative nature of nitrogen and oxygen atoms where the partial charges are  $-0.520$  and  $-0.577$  e, respectively, for **1**. All hydrogen atoms have positive partial charges while carbon atoms have negative partial charges (Figure 12). Similar results were obtained for the *bis*-pyrrolidino **3** and *bis*-piperidino **4** analogues, where the partial charges at the pyrrolidino and piperidine N-atoms are  $-0.511$  and  $-0.518$  e, respectively. The map of molecular electrostatic potential

over electron density revealed these results very well (Figure 13; MESP). On the other hand, the bromide anion has a partial charge of  $-0.703$  e in **2**, indicating some charge transfer from the bromide anion to the organic fragment. The amount of charge transference is  $0.297$  e. In this case, the red region of MESP is located over the bromide anion, while the most intense blue region is located over the protonated morpholine moiety.

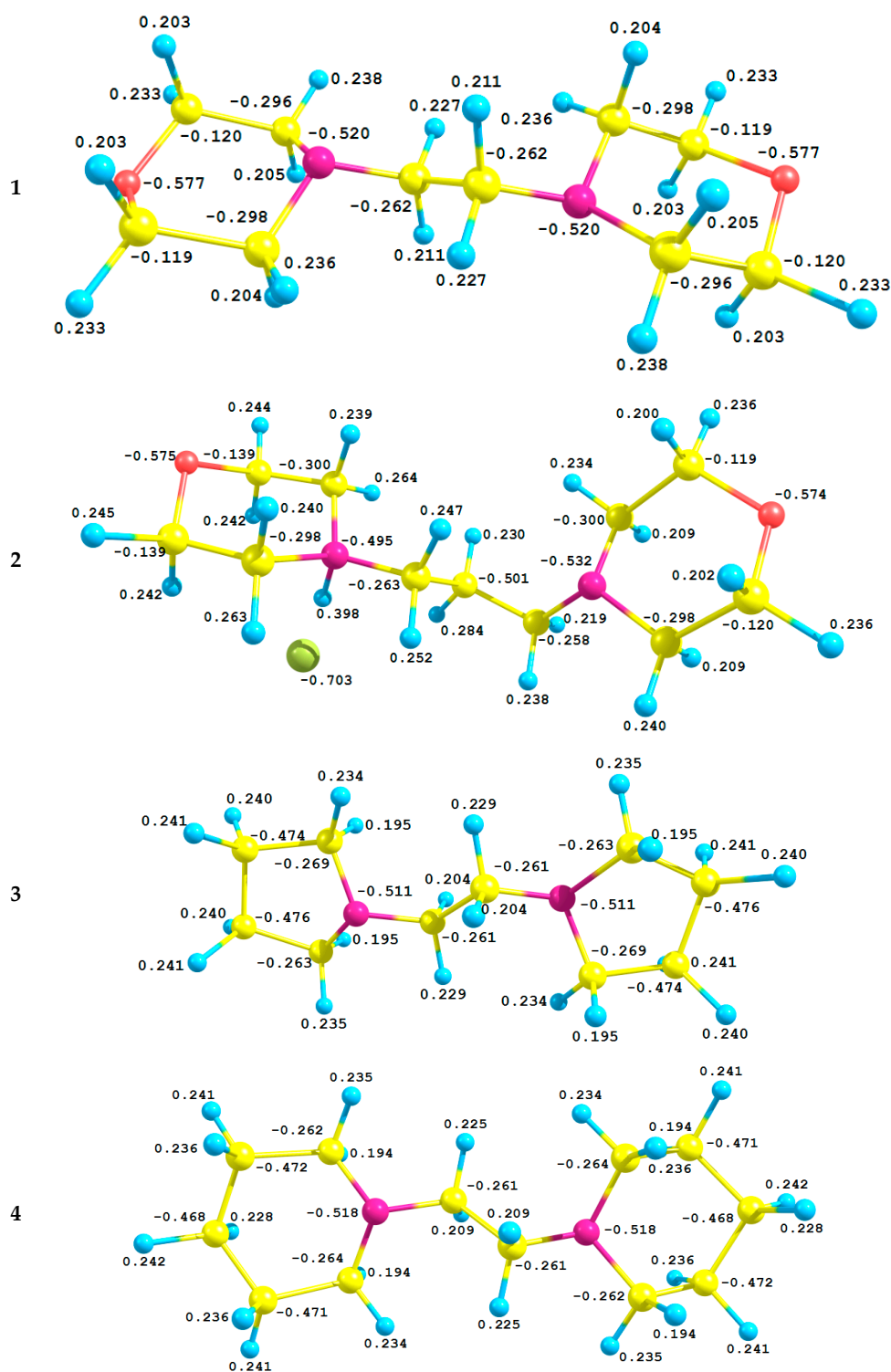
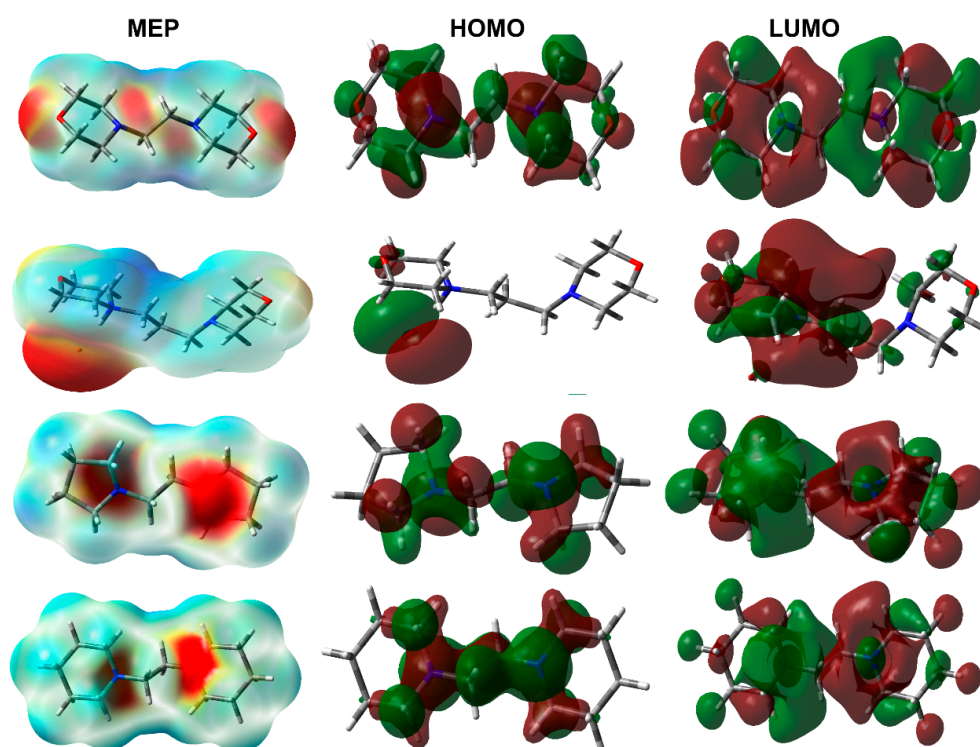


Figure 12. Partial atomic charges in the studied molecular systems.



**Figure 13.** The MESP, HOMO, and LUMO of the studied molecular systems. Compounds **1**, **2**, **3**, and **4** from up to down, respectively.

In addition, the HOMO and LUMO frontier molecular orbitals shown in Figure 12 are important for the molecule reactivity [30–36]. Their energies in case of compound **1** were calculated to be  $-5.889$  and  $2.323$  eV, respectively. The relatively high HOMO–LUMO energy gap suggests a low tendency for the system to undergo intramolecular charge transfer ( $8.212$  eV). The corresponding values in case of the *bis*-pyrrolidino-analogue **3** are  $-5.660$ ,  $2.305$ , and  $7.872$  eV, respectively. In this regard, the ionization potential (I) and electron affinity (A) for **1** are  $5.889$  and  $-2.323$  eV, respectively, while the hardness ( $\eta$ ), electrophilicity index ( $\omega$ ), and chemical potential ( $\mu$ ) are  $8.212$ ,  $0.194$ , and  $-1.783$  eV, respectively (Table 3). The corresponding values in the *bis*-pyrrolidino-analogue **3** are  $5.660$ ,  $-2.305$ ,  $7.872$ ,  $0.169$ , and  $-1.630$  eV, respectively. Similar results were obtained for compound **4**. The high stability of the system towards intramolecular charge transfer could be attributed to the absence of delocalized  $\pi$ -system, where **1** is slightly more stable than the *bis*-pyrrolidino-analogue **3**. On the other hand, the HOMO ( $-5.422$  eV) of **2** is located over the bromide ion, while the LUMO ( $1.361$  eV) is located over the protonated morpholine moiety indicating an intramolecular charge transfer from the former to the latter. The energy of this transition is  $6.783$  eV. The other reactivity descriptors for **2** are listed in the same table.

**Table 3.** Reactivity descriptors (eV) of the studied molecular systems.

Parameter	1	2	3	4
I	5.889	5.422	5.566	5.594
A	$-2.323$	$-1.361$	$-2.305$	$-2.337$
$\eta$	8.212	6.783	7.872	7.931
$\mu$	$-1.783$	$-2.031$	$-1.630$	$-1.629$
$\omega$	0.194	0.304	0.169	0.167

#### 4. Conclusions

Compounds **1** and **2** were successfully synthesized, and their structural features were assigned based on single crystal X-ray diffraction technique, while **3** and **4** were retrieved from literature for comparison with the structurally related **1**. The supramolecular structures of the studied compounds were analyzed using Hirshfeld calculations. The reactivity descriptors based on the HOMO and LUMO energies were also calculated. The calculated structures are found in good agreement with the experimentally observed X-ray structures. The molecular packing aspects and electronic properties of **1** are compared with the *bis*-pyrrolidino **3** and *bis*-piperidino **4** analogues. For **2**, there is some intramolecular charge transfer from the bromide anion as electron donor fragment to the protonated morpholine moiety as electron acceptor one. The energy of this charge transfer is 6.783 eV, and the amount of electron density transferred is 0.297 e.

**Supplementary Materials:** The following are available online at <https://www.mdpi.com/2073-8994/13/1/20/s1>. Software for X-ray determination (Tables for X-ray data); tables for computational studies; along with copies of NMR spectrum of the synthesized compounds.

**Author Contributions:** Conceptualization, A.B.; data curation, S.M.S. and M.H.; formal analysis, M.H. and M.A.; funding acquisition, A.B.; investigation, M.S.I.; A.S.A.; S.A.; methodology, M.S.I. and M.A.; software, S.M.S. and M.H.; validation, A.M.A.-M.; Visualization, A.M.A.-M.; writing—original draft, A.B. and S.M.S.; writing—review and editing, A.B. and S.M.S. All authors have read and agreed to the published version of the manuscript.

**Funding:** Deanship of Scientific Research at King Saud University for providing funding to this Research group NO (RGP-257).

**Acknowledgments:** The authors would like to extend their sincere appreciation to the Deanship of Scientific Research at King Saud University for providing funding to this Research group NO (RGP-257). The authors thank the Deanship of Scientific Research and RSSU at King Saud University for their technical support.

**Conflicts of Interest:** The authors declare no conflict of interest.

#### References

1. Singh, V.; Kaur, S.; Sapehiyia, V.; Singh, J.; Kad, G.L. Microwave accelerated preparation of [bmim][HSO<sub>4</sub>] ionic liquid: An acid catalyst for improved synthesis of coumarins. *Catal. Commun.* **2005**, *6*, 57–60. [CrossRef]
2. Zhang, R.; Meng, X.; Liu, Z.; Meng, J.; Xu, C. Isomerization of n-pentane catalyzed by acidic chloroaluminate ionic liquids. *Ind. Eng. Chem. Res.* **2008**, *47*, 8205–8210. [CrossRef]
3. Hajipour, A.R.; Rafiee, F.; Ruoho, A.E. Oxidation of benzylic alcohols to their corresponding carbonyl compounds using KIO<sub>4</sub> in ionic liquid by microwave irradiation. *Synth. Commun.* **2006**, *36*, 2563–2568. [CrossRef]
4. Hajipour, A.R.; Rafiee, F.; Ruoho, A.E. Facile and selective oxidation of benzylic alcohols to their corresponding carbonyl compounds with sodium nitrate in the presence of Brønsted acidic ionic liquids. *Synlett* **2007**, *2007*, 1118–1120. [CrossRef]
5. Bastrzyk, A.; Feder-Kubis, J. Pyrrolidinium and morpholinium ionic liquids as a novel effective destabilising agent of mineral suspension. *Colloids Surf. A* **2018**, *557*, 58–65. [CrossRef]
6. Dutta, A.; Damarla, K.; Kumar, A.; Saikia, P.J.; Sarma, D. Gemini basic ionic liquid as bi-functional catalyst for the synthesis of 2, 3-dihydroquinazolin-4 (1H)-ones at room temperature. *Tetrahedron Lett.* **2020**, *61*, 151587. [CrossRef]
7. Daniele, S.; Hubert-Pfalzgraf, L.G.; Bavoux, C. Calcium tetramethylheptanedionate adducts with N-donor ligands. Molecular structure of a dimeric and volatile adduct Ca<sub>2</sub>(η<sup>2</sup>-thd)(μ, η<sup>2</sup>-thd) 3(η<sup>2</sup>-bipy). *Polyhedron* **2001**, *20*, 1065–1070. [CrossRef]
8. Awalt, J.K.; Lam, R.; Kellam, B.; Graham, B.; Scammells, P.J.; Singer, R.D. Utility of iron nanoparticles and a solution-phase iron species for the N-demethylation of alkaloids. *Green Chem.* **2017**, *19*, 2587–2594. [CrossRef]
9. Zhang, X.; Yang, W.; Wang, L. Silver-catalyzed amidation of benzoylformic acids with tertiary amines via selective carbon–nitrogen bond cleavage. *Org. Biomol. Chem.* **2013**, *11*, 3649–3654. [CrossRef]
10. Yu, H.; Gao, B.; Hu, B.; Huang, H. Charge-transfer complex promoted C–N bond activation for Ni-catalyzed carbonylation. *Org. Lett.* **2017**, *19*, 3520–3523. [CrossRef]
11. Gao, B.; Huang, H. Palladium-catalyzed hydroaminocarbonylation of alkynes with tertiary amines via C–N bond cleavage. *Org. Lett.* **2017**, *19*, 6260–6263. [CrossRef] [PubMed]
12. Li, X.; Pan, J.; Wu, H.; Jiao, N. Rh-catalyzed aerobic oxidative cyclization of anilines, alkynes, and CO. *Chem. Sci.* **2017**, *8*, 6266–6273. [CrossRef] [PubMed]

13. Fu, Y.; Xu, Q.S.; Shi, C.Z.; Du, Z.; Xiao, C. Charge-Transfer Complex Promoted Regiospecific C–N Bond Cleavage of Vicinal Tertiary Diamines. *Adv. Synth. Catal.* **2018**, *360*, 3502–3506. [[CrossRef](#)]
14. Banks, W.A. Characteristics of Compounds That Cross the Blood-Brain Barrier. *BMC Neurol.* **2009**, *9*, S3. [[CrossRef](#)] [[PubMed](#)]
15. Mayol-Llinàs, J.; Nelson, A.; Farnaby, W.; Ayscough, A. Assessing Molecular Scaffolds for CNS Drug Discovery. *Drug Discov. Today* **2017**, *22*, 965–969.
16. Yu, L.F.; Zhang, H.K.; Caldarone, B.J.; Eaton, J.B.; Lukas, R.J.; Kozikowski, A.P. Recent Developments in Novel Antidepressants Targeting  $\alpha 4\beta 2$ -Nicotinic Acetylcholine Receptors. *J. Med. Chem.* **2014**, *57*, 8204–8223. [[CrossRef](#)]
17. Hocine, S.; Berger, G.; Hanessian, S. Design and Synthesis of Backbone-Fused, Conformationally Constrained Morpholine-Proline Chimeras. *J. Org. Chem.* **2020**, *85*, 4237–4247. [[CrossRef](#)]
18. Turner, M.J.; McKinnon, J.J.; Wolff, S.K.; Grimwood, D.J.; Spackman, P.R.; Jayatilaka, D.; Spackman, M.A. Crystal Explorer 17. University of Western Australia. 2017. Available online: <http://hirshfeldsurface.net> (accessed on 12 June 2017).
19. Frisch, M.J.; Trucks, G.W.; Schlegel, H.B.; Scuseria, G.E.; Robb, M.A.; Cheeseman, J.R.; Scalmani, G.; Barone, V.; Mennucci, B.; Petersson, G.A.; et al. *GAUSSIAN 09*; Revision A02; Gaussian Inc.: Wallingford, CT, USA, 2009.
20. Dennington, R., II; Keith, T.; Millam, J. (Eds.) *GaussView*; Version 4.1; Semichem Inc.: Shawnee Mission, KS, USA, 2007.
21. Reed, A.E.; Curtiss, L.A.; Weinhold, F. Intermolecular interactions from a natural bond orbital, donor-acceptor viewpoint. *Chem. Rev.* **1988**, *88*, 899–926. [[CrossRef](#)]
22. Otwinowski, Z.; Minor, W. Processing of X-ray Diffraction Data Collected in Oscillation Mode. In *Methods in Enzymology, Volume 276, Macromolecular Crystallography, Part A*; Carter, C.W., Sweet, J., Eds.; Academic Press: New York, NY, USA, 1997; pp. 307–326.
23. Rikagu Oxford Diffraction. *CrysAlisPro*; Agilent Technologies Inc.: Yarnton, UK, 2013.
24. Sheldrick, G.M. *SADABS—Bruker Nonius Scaling and Absorption Correction*; Bruker AXS, Inc.: Madison, WI, USA, 2012.
25. Sheldrick, G.M. *Acta Cryst.* **2015**, *C71*, 3–8.
26. Talybov, A.; Mamedbeyli, E.; Abbasov, V.; Abdullayev, Y.; Kochetkov, K. Synthesis of Substituted *N*-Alkylamines in Aqueous Media. *Green Sustain. Chem.* **2013**, *3*, 31–35. [[CrossRef](#)]
27. Katritzky, A.R.; Fan, W.; Fu, C. The chemistry of benzotriazole. A novel method for the synthesis of symmetrical vicinal tertiary and secondary diamines. *J. Org. Chem.* **1990**, *55*, 3209–3213. [[CrossRef](#)]
28. Markosyan, A.J.; Baghdasaryan, G.A.; Oganesyanyan, G.P.; Attaryan, A.O.; Asratyan, G.V. Phase-Transfer Catalyzed Alkylation of Morpholine with 1,2-Dichloroethane. *Russ. J. Gen. Chem.* **2012**, *82*, 344–345. [[CrossRef](#)]
29. Lennartson, A.; Hakansson, M. CCDC 840299: Experimental Crystal Structure Determination 2011. *CCDC* **2011**, 840299. [[CrossRef](#)]
30. Foresman, J.B.; Frisch, A.E. *Exploring Chemistry with Electronic Structure Methods*, 2nd ed.; Gaussian: Pittsburgh, PA, USA, 1996.
31. Chang, R. *Chemistry*, 7th ed.; McGraw-Hill: New York, NY, USA, 2001.
32. Kosar, B.; Albayrak, C. Spectroscopic investigations and quantum chemical computational study of (*E*)-4-methoxy-2-[(*p*-tolylimino) methyl] phenol. *Spectrochim. Acta* **2011**, *78*, 160–167. [[CrossRef](#)] [[PubMed](#)]
33. Koopmans, T.A. Ordering of wave functions and eigenenergies to the individual electrons of an atom. *Physica* **1933**, *1*, 104–113. [[CrossRef](#)]
34. Parr, R.G.; Yang, W. *Density-Functional Theory of Atoms and Molecules*; Oxford University Press: New York, NY, USA, 1989.
35. Parr, R.G.; Szentpaly, L.V.; Liu, S. Electrophilicity index. *J. Am. Chem. Soc.* **1999**, *121*, 1922–1924. [[CrossRef](#)]
36. Singh, R.N.; Kumar, A.; Tiwari, R.K.; Rawat, P.; Gupta, V.P. A combined experimental and quantum chemical (DFT and AIM) study on molecular structure, spectroscopic properties, NBO and multiple interaction analysis in a novel ethyl 4-[2-(carbamoyle)hydrazinylidene]-3, 5-dimethyl-1*H*-pyrrole-2-carboxylate and its dimer. *J. Mol. Struct.* **2013**, *1035*, 427–440. [[CrossRef](#)]